The Astrophysical Journal Letters, 781:L17 (4pp), 2014 January 20 doi:10.1088/2041-8205/781/1/L17

3XMM J185246.6+003317: ANOTHER LOW MAGNETIC FIELD MAGNETAR

N. Rea[1,2], D. Viganò[1], G. L. Israel[3], J. A. Pons[4], and D. F. Torres[1,5]

[1] Institute of Space Sciences (CSIC–IEEC), Campus UAB, Torre C5, 2a planta, E-08193 Barcelona, Spain

[2] Astronomical Institute "Anton Pannekoek," University of Amsterdam, Postbus 94249, NL-1090-GE Amsterdam, The Netherlands

[3] INAF-Astronomical Observatory of Rome, via Frascati 33, I-00040, Monte Porzio Catone, Roma, Italy

[4] Departament de Fisica Aplicada, Universitat d'Alacant, Ap. Correus 99, E-03080 Alacant, Spain

[5] Institució Catalana de Recerca i Estudis Avançats (ICREA), E-08010 Barcelona, Spain

Received 2013 November 13; accepted 2013 December 2; published 2014 January 6

ABSTRACT

We study the outburst of the newly discovered X-ray transient 3XMM J185246.6+003317, re-analyzing all available *XMM-Newton* observations of the source to perform a phase-coherent timing analysis, and derive updated values of the period and period derivative. We find the source rotating at $P = 11.55871346(6)$ s (90% confidence level; at epoch MJD 54728.7) but no evidence for a period derivative in the seven months of outburst decay spanned by the observations. This translates to a 3σ upper limit for the period derivative of $\dot{P} < 1.4 \times 10^{-13}$ s s^{-1}, which, assuming the classical magneto-dipolar braking model, gives a limit on the dipolar magnetic field of $B_{\rm dip} < 4.1 \times 10^{13}$ G. The X-ray outburst and spectral characteristics of 3XMM J185246.6+003317 confirm its identification as a magnetar, but the magnetic field upper limit we derive defines it as the third "low-B" magnetar discovered in the past 3 yr, after SGR 0418+5729 and Swift J1822.3−1606. We have also obtained an upper limit to the quiescent luminosity ($<4 \times 10^{33}$ erg s^{-1}), in line with the expectations for an old magnetar. The discovery of this new low field magnetar reaffirms the prediction of about one outburst per year from the hidden population of aged magnetars.

Key words: pulsars: general – X-rays: stars

Online-only material: color figures

1. INTRODUCTION

Neutron stars are the relic of the supernova explosions of massive stars (Baade & Zwicky 1934). Five decades after their discovery (Hewish et al. 1968), these compact objects have appeared in many different forms. The most common are radio pulsars, usually modeled as rapidly rotating magnetic dipoles. Another important subgroup is formed by binary neutron stars, either as X-ray pulsars accreting from a companion or normal radio pulsars orbiting a companion star. Perhaps the most intriguing class among isolated neutron stars are the "magnetars," so called because they are believed to be powered by their super strong magnetic field (see Mereghetti 2008; Rea & Esposito 2011 for recent reviews). Initially classified as anomalous X-ray pulsars and soft gamma repeaters (SGRs), it is now accepted that this is not an intrinsic distinction but rather a historical nomenclature due to the different ways they were discovered: as a steady emitter visible in X-ray surveys or during a high-energy burst or flare from a new direction in the sky. Magnetars are characterized by rotational periods in the 0.3–12 s range, period derivatives between 10^{-15}–10^{-10} s s^{-1}, X-ray luminosities of 10^{31}–10^{35} erg s^{-1}, and episodes of enhanced X-ray persistent emission either as a long-lived radiative outburst (lasting months–years) or short bursts and flares (lasting seconds–minutes). Both their steady and transient X-ray phenomena are powered by their strong magnetic fields that can stress the neutron star crust causing stellar quakes, accompanied by global magnetospheric reorganizations with the subsequent powerful high-energy emission. Eventually, shorter flares might instead be purely magnetospheric, caused by reconnection of magnetic field lines higher up in the magnetosphere (Thompson et al. 2002; Lyutikov 2003).

In 2009, a peculiar magnetar (van der Horst et al. 2010; Esposito et al. 2010; Rea et al. 2010) was discovered during an active epoch (SGR 0418+5729) as have many other members of the magnetar class, but in this case, its estimated surface dipolar magnetic field (at the equator) of $B = 6.2 \times 10^{12}$ G (Rea et al. 2013) was rather low, more typical of a normal radio pulsar. Some years later, another "low magnetic field magnetar" was discovered (Swift J1822.3−1606 : $B \sim 2 \times 10^{13}$ G; Rea et al. 2012; Scholz et al. 2012), again showing all of the characteristics of the outburst activity of a typical magnetar. A plausible solution to the apparent puzzle considers these objects as aged magnetars that have largely dissipated their external dipolar field but still hold a crustal/internal field one or two orders of magnitude larger. This internal field would be responsible for the bursting activity and intense outbursts (Rea et al. 2010; Turolla et al. 2011). This scenario has been strengthened by detailed studies of the evolution of neutron stars endowed with strong magnetic fields, and applied to the two known low field magnetars (Pons et al. 2009; Viganò et al. 2013; Rea et al. 2013). Furthermore, the absorption feature observed during the outburst of the lowest field magnetar, SGR 0418+5729, if interpreted as a proton cyclotron feature, confirms a $\sim 10^{14}$ G magnetic field in a magnetic loop close to the surface (Tiengo et al. 2013).

In this Letter, we have re-analyzed all the archival *XMM-Newton* observations of 3XMM J185246.6+003317 (hereafter 3XMM J1852+0033): a new transient source discovered serendipitously while undergoing an outburst in 2008 (Zhou et al. 2014). We first report on the data analysis, and in Section 5, we argue that this source is a low magnetic field magnetar and discuss the consequences of this finding in terms of the population of old magnetars and their magneto-thermal evolutionary path.

2. *XMM-NEWTON* DATA ANALYSIS

3XMM J1852+0033 was observed several times with *XMM-Newton* (Jansen et al. 2001). Data have been processed using *SAS* version 13, and we have employed the most updated calibration files available at the time the reduction was performed (2013

Table 1
Summary of the *XMM-Newton* Observations

ObsID	Obs. Date (YYYY MM DD)	Camera	Exposure (ks)	Count Rate (count s^{-1})
		Quiescence		
0204970201	2004 Oct 18	MOS2	31.4	<0.004
		MOS1	31.4	<0.005
0204970301	2004 Oct 24	MOS2	31.1	<0.004
		MOS1	31.4	<0.005
0400390201	2006 Oct 8	MOS2	30.4	<0.005
0400390201	2007 Mar 20	MOS2	34.4	<0.007
		MOS1	34.4	<0.006
		Outburst		
0550670201	2008 Sep 19	MOS2	21.6	0.210 ± 0.003
0550670301	2008 Sep 21	MOS2	30.3	0.199 ± 0.003
0550670401	2008 Sep 23	MOS2	35.4	0.196 ± 0.003
0550670501	2008 Sep 29	MOS2	33.3	0.198 ± 0.003
0550670601	2008 Oct 10	MOS2	35.5	0.148 ± 0.002
0550671001	2009 Mar 16	MOS2	27.2	0.033 ± 0.001
		MOS1	27.2	0.033 ± 0.001
0550670901	2009 Mar 17	MOS2	26.2	0.030 ± 0.001
		MOS1	26.2	0.033 ± 0.001
0550671201	2009 Mar 23	MOS2	27.1	0.030 ± 0.001
		MOS1	27.1	0.032 ± 0.001
0550671101	2009 Mar 25	MOS2	18.8	0.028 ± 0.002
		MOS1	19.6	0.033 ± 0.001
0550671301	2009 Apr 4	MOS2	26.2	0.013 ± 0.007
		MOS1	26.2	0.028 ± 0.001
0550671901	2009 Apr 10	MOS2	30.7	0.023 ± 0.001
		MOS1	30.6	0.024 ± 0.001
0550671801	2009 Apr 22	MOS2	28.2	0.026 ± 0.001
		MOS1	28.2	0.024 ± 0.001

November). The source was detected serendipitously only in the Metal Oxide Semiconductor (MOS) cameras (Turner et al. 2001; see Table 1) in the 2008 and 2009 observations. The MOS1 and MOS2 cameras were set up in full frame mode, with a timing resolution of 2.6 s. We have applied standard data screening criteria in the extraction of scientific products. Source photons were extracted from a circular region with a radius of 40″, and a similar circle was used for the background, in the same CCD of the source. We used the same extraction region to estimate the count rate upper limit for the four observations of the source in quiescence (see Table 1). Our spectral analysis was restricted to photons having PATTERN $\leqslant$ 12 and FLAG = 0. All photon arrival times have been referred to the solar system barycenter (TDB time system and DE200 ephemeris).

3. OUTBURST

3.1. Timing Analysis

Timing analysis was performed using the phase-fitting technique (details on this technique can be found in Dall'Osso et al. 2003), and using all "outburst" data listed in Table 1 (both from the MOS1 and MOS2 cameras when available). We merged the photon arrival times of some contiguous pointings (2008 September 19–29, 2009 March 16–25, and 2009 April 4–22) in order to increase the phase accuracy and/or to reduce the datapoint scatter (see Figure 1). Data were folded using a trial period of 11.5587072 s at epoch 54728.7 MJD. The phase of the modulation was inferred by fitting the average pulse shape of each observation (folded with the above trial period), with one or more harmonics (the exact number was determined by requesting that the inclusion of any higher harmonic was statistically significant). In almost all cases, the use of the fundamental harmonic alone was sufficiently accurate. In Figure 1, we plot the phases at which the fundamental sine function fitted to the pulse profile is equal to zero.

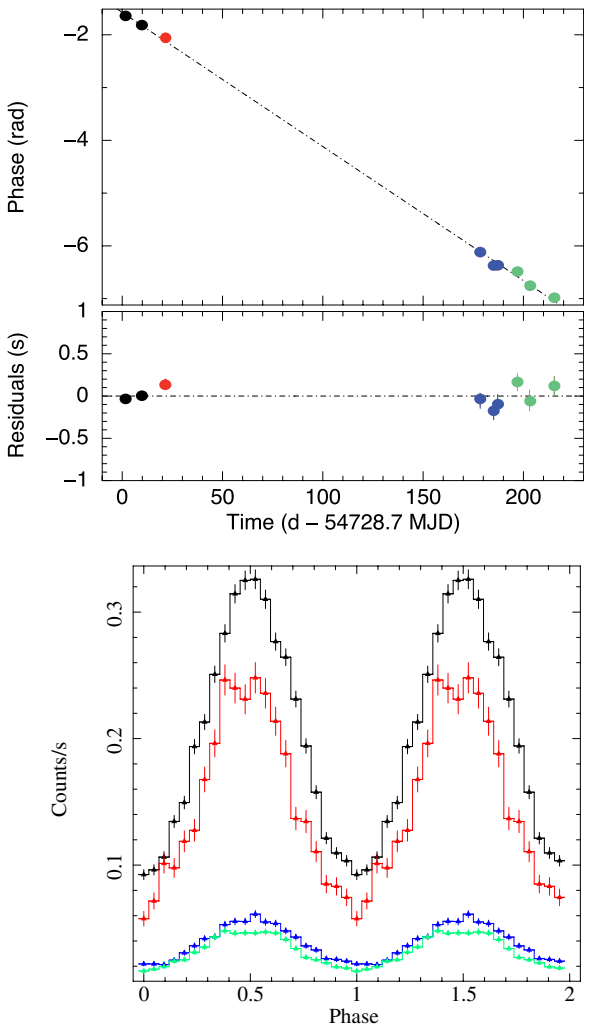

Figure 1. Left: 3XMM J1852+0033's pulse phases derived by fitting with a sine function the pulse profile folded with a trial period (see text for details, and below for the color code definition). The phase evolution in time is fitted with a linear function. The residuals with respect to our best phase-coherent solution are reported in the lower panel, in units of seconds. Right: pulse profiles in the 0.3–10 keV energy range. From top to bottom they refer to: (1) black—MOS2 observations performed between 2008 September 19–29, with a 0.5–10 keV observed flux of $\sim 4.2 \times 10^{-12}$ erg $s^{-1}cm^{-2}$ (see also Figure 2), (2) red—2008 October 10 (MOS2) at a flux of $\sim 2.8 \times 10^{-12}$ erg $s^{-1}cm^{-2}$, (3) blue—2009 March 16–25 (MOS1 and MOS2) at $\sim 6 \times 10^{-13}$ erg $s^{-1}cm^{-2}$, and (4) green—2009 April 4–22 (MOS1 and MOS2) at $\sim 5 \times 10^{-13}$ erg $s^{-1}cm^{-2}$ (note that some observations have been merged to increase the accuracy in the phase determination).

(A color version of this figure is available in the online journal.)

The time evolution of the phase can be described by a relation: $\phi = \phi_0 + 2\pi(t - t_0)/P - \pi(t - t_0)^2 \dot{P}/P^2$. A linear fit of the resulting pulse phases, by assuming the initial trial period reported above, gives a reduced $\chi^2_r \sim 2$ for 8 degrees of freedom (dof hereafter). The inclusion of a quadratic term in the phase modeling, corresponding to a first period derivative component, was not significant in our data with a 3σ (two parameters of interest, p.o.i) upper limit on the period derivative of $\dot{P} < 1.4 \times 10^{-13}$ s s^{-1} and a reduced $\chi^2_r \sim 2.2$ (for 7 dof; see also Figure 1). The resulting best-fit solution corresponds to a spin period of $P = 11.55871346(6)$ s (90%

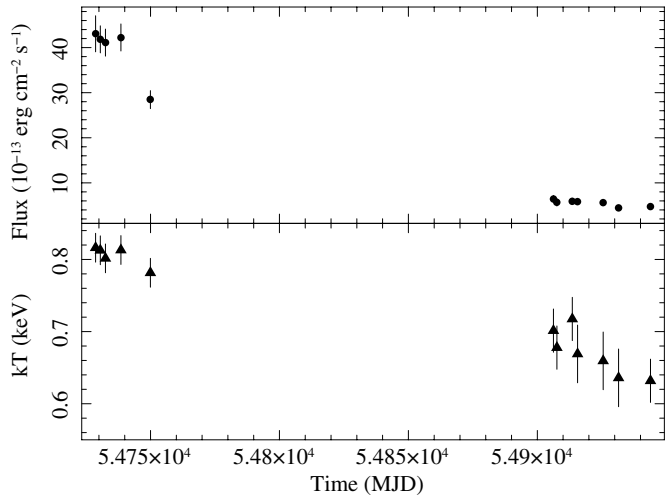

Figure 2. Evolution of the 0.5–10 keV observed flux and blackbody temperature as a function of time (see text for details).

confidence level and 1 p.o.i; epoch 54728.7 MJD). The new timing solution implies a rms variability of <0.2 s.

The pulse profile seems rather stable in shape, a single peak remaining in phase during the outburst decay. However, we note that we caught the outburst at a late time, and a pulse profile stabilization was already observed in other low-B magnetars during the outburst decay. The pulsed fraction is relatively stable in time with an average value of ∼62% (defined as the semi-amplitude of the fundamental sinusoidal modulation divided by the mean source count rate).

3.2. Spectral Analysis

We have performed the spectral analysis using all of the observations during the outburst phase of 3XMM J1852+0033 reported in Table 1, and data from both the MOS1 and MOS2 cameras when available. Spectra from the 2008 observations were grouped to have at least 50 counts per bin, while for the 2009 observations, we required at least 30 counts per bin. The rebinning was made with special care in order not to oversample the instrument spectral resolution by more than a factor of three. We used XSPEC 12.7.1 for the spectral fitting. Our results are consistent within errors with those of Zhou et al. (2014). We report in Figure 2, the evolution of the spectral parameters and of the 0.5–10 keV observed flux for a `phabs*bbodyrad` spectral model ($\chi^2 = 1.1$ (1049 dof); $N_{\rm H} = 1.32(5) \times 10^{22}$ cm^{-2}). Similar to Zhou et al. (2014), we find a tiny excess flux at energies higher than 6 keV which is not properly modeled by a single blackbody model alone (although this is not influencing the goodness of the χ^2). Using a resonant cyclotron scattering (RCS) model (Rea et al. 2008), this excess is instead well accounted for (note, however, that the RCS has two additional free parameters) by the nonthermal scattering tail. We refer to Zhou et al. (2014) for other details about the spectral parameters inferred by this model. Assuming a distance of 7.1 kpc, we find a blackbody radius decreasing from 0.8 km to 0.4 km.

4. QUIESCENCE

In order to derive a stringent upper limit to the flux of 3XMM J1852+0033 during its quiescent state, we have extracted all photons encircled in a 40″ radius around the position of the source, for the four available observations (Table 1) and both the MOS1 and MOS2 cameras when available. We have added all of the event files of the MOS1 and MOS2, created an image of the resulting merged event file, and used the `Ximage` *sosta* tool to derive a source upper limit taking into account its point-spread function correction for the off-axis position, the vignetting, and the sampling dead time. This method uses the Bayesian approach with the prior function set to the prescription described in Kraft et al. (1991). We have derived, for a total exposure time of 251 ks, a 3σ upper limit on the source count rate of 0.0014 count s^{-1} in the 0.3–10 keV range. With this upper limit, assuming a distance of 7.1 kpc, a 10 km radius surface emission, and an $N_{\rm H} = 1.32 \times 10^{22}$ cm^{-2} (as derived in Section 3.2), we can obtain the upper limits on the surface temperature and on the bolometric thermal luminosity during quiescence of kT < 0.15 keV, and $L_{\rm qui} < 4 \times 10^{33}$ erg s^{-1}.

5. DISCUSSION

We have reported a phase-coherent timing solution for the newly discovered transient 3XMM J1852+0033 (Zhou et al. 2014), which underwent an outburst in 2008, and was caught serendipitously by *XMM-Newton* during a series of observations of the supernova remnant (SNR) Kes 79 and its central compact object CXOU J1852+0040 (Seward et al. 2003; Halpern & Gotthelf 2010). The spin period does not show any sign of Doppler shifts due to a possible companion star (and no companion star is observed in the optical or infrared bands in the available catalogs; Zhou et al. 2014). Assuming that the pulsar is isolated, its rotational properties indicate a dipolar surface magnetic field (at the equator) of $B = 3.2 \times 10^{19}(P\dot{P})^{1/2} < 4 \times 10^{13}$ G, and the characteristic age and the rotation power are $\tau_c = P/(2\dot{P}) > 1.3$ Myr and $\dot{E}_{\rm rot} = 3.9 \times 10^{46} \dot{P}/P^{-3} < 3.5 \times 10^{30}$ erg s^{-1}, respectively. Despite the relatively low dipolar magnetic field, the detection of an outburst and the observed spectral characteristics confirm the magnetar nature of this transient source.

In Figure 3, we show the expected timing and luminosity evolution for isolated neutron stars born with a dipolar field intensity (at the pole) between $B = 10^{14}$ G and $B = 10^{15}$ G. The expected properties are in line with the observed properties of all high-B pulsars, X-ray emitting isolated neutron stars (XINSs) and magnetars.[6] As the right panel shows, 3XMM J1852+0033 is compatible with the expected evolution of a neutron star born with an initial dipolar magnetic field (at the pole) of $B \sim 3$–4×10^{14} G, which is now at the same evolutionary stage as the other low-B magnetars, hence about an Myr. In particular, except for the occasional outburst, the long spin period, $P \sim 11.57$ s, and the relatively low quiescent luminosity, $L_{\rm qui} < 4 \times 10^{33}$ erg s^{-1}of 3XMM J1852+0033 (and of the other low-B magnetars SGR 0418+5729 and Swift J1822.3−1606; Rea et al. 2012, 2013; Scholz et al. 2012) would place it in the same class as the XINS, a group of nearby, thermally emitting isolated neutron stars with typical temperatures of 0.1 keV. The possibility that XINS or some of the other high-B pulsars are simply aged, less active magnetars has been proposed and tested in the last few years (see, e.g., Pons & Perna 2011; Viganò et al. 2013; Rea et al. 2013, and references therein).

In this scenario, 3XMM J1852+0033 lies on the same evolutionary track as the large group of other 6–7 neutron stars (magnetars and XINSs), perhaps indicating a common,

[6] Note that the high luminosity of some young magnetars is likely to be partly due to the contribution of the magnetospheric plasma, which yields part of its kinetic energy to X-ray photons via RCS. Thus, it is hard to infer the purely thermal component in the X-ray spectrum; see Viganò et al. (2013) for details.

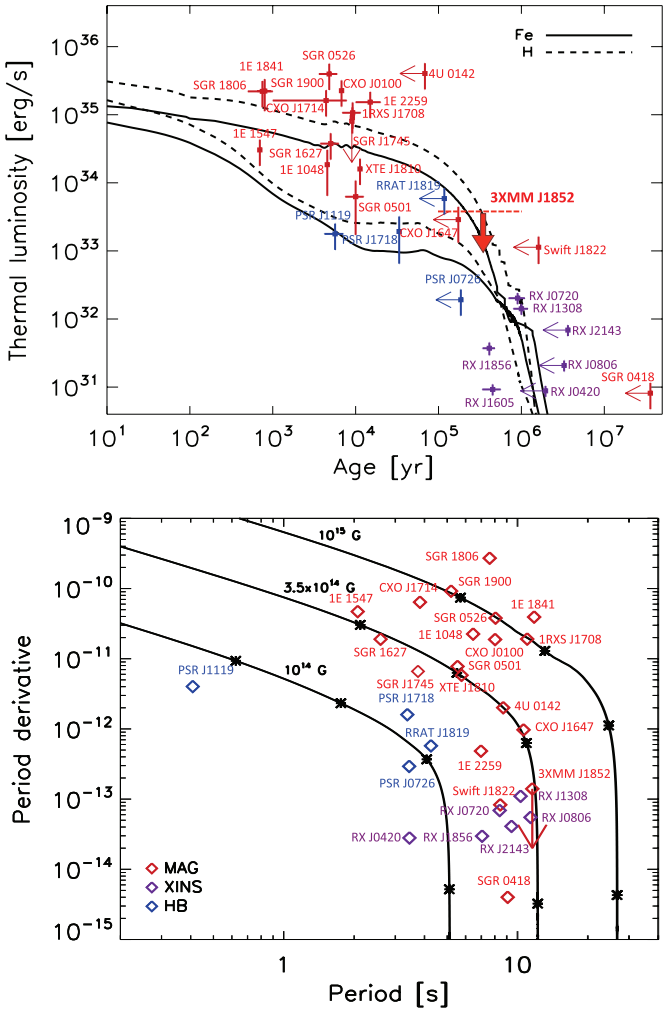

Figure 3. Comparison between observed properties of magnetars (red), high B pulsars (blue), and XINSs (purple), and the predictions from magneto-thermal models (lines, see Viganò et al. 2013 for details about both observed and predicted values). Left: quiescent bolometric thermal luminosity vs. age for an isolated neutron star born with a dipolar field (at the pole) of $B = 10^{14}$ (top lines) and $B = 10^{15}$ G (lower lines), for an iron (solid) or hydrogen envelope (dashed). Arrows indicate sources with no available alternative age estimate (e.g., SNR age) and large characteristic ages, which very likely overestimate the real age due to magnetic field dissipation. The limit we derive 3XMM J1852+0033's quiescent luminosity is indicated with a red arrow, and the dashed line represents the limits on the magneto-thermal age (see text for details). Right: evolution of the timing properties for $B = 10^{14}$ G, $B = 3.5 \times 10^{14}$ G, and $B = 10^{15}$ G, assuming an aligned rotator in the spin-down formula by Spitkovsky (2006). Asterisks indicate the real ages of 1, 10, 100, and 500 kyr in descending order along the magnetic isotracks.

(A color version of this figure is available in the online journal.)

typical initial magnetic field for these magnetars. The upper limit of $\dot{P}$ can be translated, within our evolutionary model, into a lower limit on the age of $\gtrsim$100 kyr. In our theoretical models, sporadical outbursts are expected to occur until a maximum age of $\sim$1 Myr, after which the magnetic field is too weak to cause any significant crustal fracture. Thus, we can roughly estimate the real age between $\sim$0.1–1 Myr (see also Figure 3, left panel). The upper limit we obtained for the quiescence luminosity is also compatible with the theoretical expectations for the age of $\sim10^{32}$–10^{33} erg s^{-1} (see left panel of Figure 3). 3XMM J1852+0033 has the second largest period among isolated X-ray neutron stars, after 1E 1841–045, which confirms the clustering of periods of magnetars and XINS in a narrow range, not exceeding $\sim$12 s, and reinforces the idea that there must be a physical mechanism limiting the spin period (Pons et al. 2013).

In summary, all the outburst characteristics of 3XMM J1852+0033 are typical of magnetars (Rea & Esposito 2011), with the outburst decay compatible with the crustal cooling scenario. This discovery supports the scenario in which magnetar-like activity is also expected in *normal* neutron stars, with inferred dipolar fields lower than the typical magnetar strength, 10^{14}–10^{15} G. A stronger crustal/internal field can be responsible for the bursting activity of these aged magnetars (Rea et al. 2010, 2013; Turolla et al. 2011), although with a much lower event rate (less than $\sim$ one outburst per millennium; see Perna & Pons 2011) than younger objects. A simple estimate (see the discussion in Section 8.2 of Rea et al. 2013) gives an expected outburst rate for the entire population of low-B magnetars in the galaxy of $\approx$1 yr^{-1}. This number has to be confirmed by more detailed population synthesis studies including possible observational biases and selection effects, but it would not be surprising that more and more of these events are observed (or found in archival data after a more careful revision) in the upcoming years.

Our last remark is about the possible association to the SNR Kes 79. Despite their apparent vicinity and a similar value of $N_{\rm H}$, this SNR is estimated to be $\sim$5–7 kyr old (Sun et al. 2004), much younger than the magnetar, and it hosts the CCO J1852+0040. Therefore, we find a possible association between the magnetar and Kes 79 unlikely.

N.R. is supported by a Ramón y Cajal fellowship and by an NWO Vidi award. N.R., D.V., and D.F.T. acknowledge support from grants AYA2012-39303, SGR 2009-811, and iLINK 2011-0303. J.A.P. acknowledges support from the grants AYA 2010-21097-C03-02 and Prometeo/2009/103. We thank Paolo Esposito for suggestions about the usage of the `sosta` Ximage tool, Sergei Popov for pointing out a misreference in a draft version of this Letter, and the referee for useful suggestions.

REFERENCES

Baade, W., & Zwicky, F. 1934, PNAS, 20, 254
Dall'Osso, S., Israel, G. L., Stella, L., et al. 2003, ApJ, 599, 485
Esposito, P., Israel, G. L., Turolla, R., et al. 2010, MNRAS, 405, 1787
Halpern, J. P., & Gotthelf, E. V. 2010, ApJ, 709, 436
Hewish, A., Bell, S. J., Pilkington, J. D. H., et al. 1968, Natur, 217, 709
Jansen, F., Lumb, D., Altieri, B., et al. 2001, A&A, 365, L1
Kraft, R. P., Burrows, D. N., & Nousek, J. A. 1991, ApJ, 374, 344
Lyutikov, M. 2003, MNRAS, 346, 540
Mereghetti, S. 2008, A&ARv, 15, 225
Perna, R., & Pons, J. A. 2011, ApJL, 727, L51
Pons, J. A., Miralles, J. A., & Geppert, U. 2009, A&A, 496, 207
Pons, J. A., & Perna, R. 2011, ApJ, 741, 123
Pons, J. A., Viganò, D., & Rea, N. 2013, NatPh, 9, 431
Rea, N., & Esposito, P. 2011, in High-Energy Emission from Pulsars and Their Systems, ed. D. F. Torres & N. Rea (Berlin: Springer), 247
Rea, N., Esposito, P., Turolla, R., et al. 2010, Sci, 330, 944
Rea, N., Israel, G. L., Esposito, P., et al. 2012, ApJ, 754, 27
Rea, N., Israel, G. L., Pons, J. A., et al. 2013, ApJ, 770, 65
Rea, N., Zane, S., Turolla, R., Lyutikov, M., & Götz, D. 2008, ApJ, 686, 1245
Scholz, P., Ng, C.-Y., Livingstone, M. A., et al. 2012, ApJ, 761, 66
Seward, F. D., Slane, P. O., Smith, R. K., et al. 2003, ApJ, 584, 414
Spitkovsky, A. 2006, ApJL, 648, L51
Sun, M., Seward, F. D., Smith, R. K., et al. 2004, ApJ, 605, 742
Thompson, C., Lyutikov, M., & Kulkarni, S. R. 2002, ApJ, 574, 332
Tiengo, A., Esposito, P., Mereghetti, S., et al. 2013, Natur, 500, 312
Turner, M. J. L., Abbey, A., Arnaud, M., et al. 2001, A&A, 365, L27
Turolla, R., Zane, S., Pons, J. A., et al. 2011, ApJ, 740, 105
van der Horst, A. J., Connaughton, V., Kouveliotou, C., et al. 2010, ApJL, 711, L1
Viganò, D., Rea, N., Pons, J. A., et al. 2013, MNRAS, 434, 123
Zhou, P., Chen, Y., Li, X.-D., et al. 2014, ApJL, 781, L16